Journal of Optoelectronics and Advanced Materials, Vol. 7, No. 1, February 2005, p. 107 - 114

Invited Paper

COMPUTER MODELLING OF MULTI-TRAPPING AND HOPPING TRANSPORT IN DISORDERED SEMICONDUCTORS

C. Main*, J. M. Marshall[a], S. Reynolds[b]

University of Dundee, Division of Electronic Engineering and Physics, Nethergate, Dundee DD1 4HN
[a]University of Wales Swansea, Singleton Park, Swansea SA2 8PP, United Kingdom
[b]University of Abertay Dundee, School of Computing and Advanced Technologies, Bell Street, Dundee DD1 1HG, United Kingdom

In this paper we demonstrate a simple computational procedure for the simulation of transport in a disordered semiconductor in which both multi-trapping and hopping processes are occurring simultaneously. We base the simulation on earlier work on hopping transport, which used a Monte-Carlo method. We use the same model concepts, but employ a stochastic matrix approach to speed computation, and include also multi-trapping transitions between localised and extended states. We use the simulation to study the relative contributions of extended state conduction (with multi-trapping) and hopping conduction (via localised states) to transient photocurrents, for various distributions of localised gap states, and as a function of temperature. The implications of our findings for the interpretation of transient photocurrents are examined.

(Received December 9, 2004; accepted January 26, 2005)

Keywords: Hopping transport, Disordered semiconductors, Computer simulation.

1. Introduction

The transient electronic properties of disordered semiconductors, manifested in, for example, the photocurrent response (TPC) following excitation by a short laser pulse are determined by a combination of carrier transport processes. The non-equilibrium distribution of excess carriers created by such a pulse will diffuse and drift while relaxing in energy toward thermal equilibrium. If the 'post-pulse' excess carriers initially exist in extended states, their relaxation and transport will involve the participation of localised states either by 'multi-trapping' (MT) processes in which transitions occur only between localised and extended states, or by direct inter-site tunnelling or 'hopping'. In the former case, any measured current arises from trap-limited band transport, whilst in the latter case the current arises from hopping transport.

Numerous analytical studies have been made of such a transient photoresponse, when one or other of these processes is dominant [1,2]. Earlier studies focussed mainly on specific distributions of states, such as exponential band-tails, for simplicity. More recently, analysis with the aid of computer modelling has allowed the study of more general cases of arbitrary distributions of states. In particular, techniques have been developed by the present authors to reveal, in a *spectroscopic* fashion, information on the energy distribution of localised states (DOS) from measurements of the transient photocurrent decay [3], assuming that MT processes dominate transport. Marshall [4] has studied, by computer modelling applicable to an arbitrary DOS, the case of transient photocurrents in the case of hopping transport, employing Monte-Carlo techniques.

* Corresponding author: charlie.main@gmail.com

In this paper we use the approach described by Marshall [4,5], but we now include both MT and hopping processes. Additionally, we replace the Monte-Carlo solution of the rate equations describing carrier relaxation with a matrix-based Markov chain computation, adapted to deal with extremely wide time intervals which can cause difficulties with the 'stiff' equation systems often encountered in such studies. This paper outlines the development of this solution method, and presents results of its application to several illustrative DOS cases, following the simultaneous evolution of transient MT and hopping transport. We firstly examine the case of a broad exponential tail, and then two cases of localised state distributions which represent a 'standard' a-Si:H DOS and a high-defect a-Si:H case. Further, we analyse the effect of application of the DOS analysis developed for the MT case, in the present case where such 'combined' transport may occur.

2. Modelling of transport

Following Marshall [4], we represent the continuous distribution $g(E)$ of localised states by a 'ladder' of states grouped into slices of energy width ΔE. Thus, the level 'i' of this discretised distribution has an approximate density $g(E_i)\Delta E$ cm^{-3}. Marshall pointed out that since the mean inter-site spacing $\bar{r}_i$ for any given slice i, is given by $\bar{r}_i = \left(g(E_i)\Delta E\right)^{-1/3}$, the computed nearest – neighbour hopping rate can depend on the value of ΔE chosen, and presented procedures which address this problem. We will not further explore such procedures here, but will employ one – the 'fractional' approach, outlined briefly below.

Firstly, we write the probability of hops to iso-energetic or deeper sites at energy E_j from a site at energy E_i as

$$p_{i,j} = \upsilon_0 \left(g(E_j)\Delta E / N_{i,deep} \right) \exp\left(- r_{i,deep} / 2R_0 \right), \tag{1}$$

where ν_0 is an attempt-to-hop frequency, $N_{i,deep} = \int_{E_i}^{\infty} g(E)dE \approx \sum_k g(E_k)\Delta E \quad (k \geq i)$ is the total number of iso-energetic and deeper sites, with corresponding mean separation $r_{i,deep} = \left(N_{i,deep}\right)^{-1/3}$, and R_0 is a localisation parameter for the sites. In this paper, we restrict R_0 to a value of 5×10^{-8} cm, in the middle of the expected range; variations will be examined in later work. The ratio $g(E_j)\Delta E / N_{i,deep}$ represents the fraction of all such sites in slice 'j', since the probability of hopping to a given slice is proportional to the fractional concentration of sites it contains. For hops upward in energy, from a site in a deeper slice at energy E_j up to E_i, detailed balance gives the inverse hop probability

$$p_{j,i} = p_{i,j} \left(g(E_i) / g(E_j) \right) \exp\left(- \left(E_j - E_i \right) / kT \right), \tag{2}$$

where kT is the thermal energy.

Multi-trapping transition probabilities may similarly be written, for trapping of a carrier in the conduction band by a trap in slice 'i',

$$p_{c,i} = \left(\upsilon / N_C \right) g(E_i)\Delta E , \tag{3}$$

while for the inverse process, thermal re-emission, the expression is

$$p_{i,c} = \upsilon \exp\left(- \left(E_C - E_i \right) / kT \right), \tag{4}$$

where ν is an attempt-to escape frequency, N_C is the effective density of states in the conduction band, and E_C is the mobility-edge energy. We assume that the occupancy of states is always low, so that the system may be assumed linear.

Rather than use the above probabilities in a Monte-Carlo simulation, as outlined in Marshall [4], they may be incorporated into a set of rate equations describing the time dependence of the densities of electrons in both localised and extended states. With appropriate initial conditions, such as the introduction of excess free or localised carriers, these will describe the progress of carrier relaxation in for example, a transient photocurrent experiment. The rate equations are as follows:

$$\frac{dn}{dt} = -n\sum_i p_{c,i} + \sum_i n_{ti}\, p_{i,c} \tag{5}$$

$$\frac{dn_{ti}}{dt} = np_{c,i} - n_{ti}\, p_{i,c} + \sum_j n_{tj}\, p_{j,i} - n_{ti}\sum_j p_{i,j}\ , \tag{6}$$

where n is the instantaneous density of free electrons, and n_{ti} is the density of electrons on sites in slice 'i'. In the following, we will assume that there are 'M' levels, including the conduction band.

To perform a discrete 'time-stepping' numerical solution, we can use these equations to compute updated values of each of the variables n, n_{ti},… as time is incremented by a step Δt, using previous values of the variables. Re-casting the above equations in matrix-vector form, we obtain

$$\mathbf{n}(t+\Delta t) = \mathbf{A}.\mathbf{n}(t), \tag{7}$$

where $\mathbf{n}(t)$ is the vector of the instantaneous free and localised carrier densities, and $\mathbf{A}$ is an $M\times M$ 'stochastic' transition matrix with elements

$$A_{1,1} = 1-\sum_{i=2}^{M} p_{c,i}\Delta t\,, \qquad A_{i,1} = p_{c,i}\Delta t\,, \qquad A_{1,i} = p_{i,c}\Delta t\,, \tag{8a,b,c}$$

$$A_{i,i} = 1-\left(p_{i,c} + \sum_{j=2}^{M} p_{i,j} - p_{i,i}\right)\Delta t \quad , \qquad A_{i,j} = p_{j,i}\Delta t \quad j\neq i\,. \tag{8d,e}$$

It is important to note that the system of equations Eq. 5 and Eq. 6 is 'stiff'. In practice this means that time step Δt cannot exceed the shortest time-constant of the system, in this case, the overall trapping time of free carriers into the ensemble of traps $\tau_{trap} = \left(\sum_i p_{c,i}\right)^{-1}$. It is clear that if $\Delta t > \tau_{trap}$, then more than 100% of free carriers would be trapped in a time-step, a physical impossibility, and a cause of terminal instability in the solution. This is a standard problem with such 'explicit' time-stepping methods, which extrapolate from present to future values. Since this trapping time is of order 1ps, then it is unfeasible to attempt to simulate the system response over time scales which, under experimental conditions, can extend up to 100s.

It is possible to deal with such systems using stable 'implicit' numerical methods, and the authors have done so in previous work on MT simulation [6]. However, in the present case, there is a simple artifice, which allows the explicit formulation described above, to be used to follow the time evolution of the system over very long time-spans. Using a suitably small value for Δt of 10^{-14} s, we can, by continued squaring of the matrix $\mathbf{A}$, generate very long effective time steps, *viz*-

$$\mathbf{n}(t+2^m\Delta t) = \mathbf{A}^{2^m}.\mathbf{n}(t). \tag{9}$$

In this way, we may extend the simulation time-scale from 10^{-14}s to 10^{+6}s, in only 72 steps, although extended-precision arithmetic is required to minimise truncation errors. Initial conditions for the simulation of TPC, with MT-only transport or MT+hopping, are determined by setting the leading element of vector $\mathbf{n}(0)$ to a normalised value of *e.g.*, 1.0, and all other elements to zero.

Computation of the transient current is more problematic; for free carriers, we may simply compute the instantaneous extended state conductivity $\sigma_{ext} = nq\mu_{ext}$, where q is the electronic charge and μ_{ext} is the free carrier mobility. For hopping carriers, and for low fields, Marshall has examined a number of approximate procedures based on computing the effective diffusivity of carriers in each slice, as determined by the hop rate from sites in a given slice, and some 'average' hop distance. All give similar results, and we use here the simplest – that of taking the hop distance from slice '*i*' to slice '*j*' as the mean separation of sites in slice '*j*', *viz.*, $\bar{r}_j = \left(g(E_j)\Delta E\right)^{-1/3}$. This yields a hop distance which is weakly dependent on slice width, and which has a (small) number of long hops to very deep states. We refer the reader to Marshall [4] for an examination of several such approximate methods.

The contribution σ_i of each level to the hopping conductivity, and the total hopping conductivity σ_{hop} may then be found, after application of the Einstein relation giving,

$$\sigma_i = n_{ti} q^2 \sum_j p_{i,j} \bar{r}_j^{\,2} / 6kT \,, \tag{10}$$

$$\sigma_{hop} = \sum_i n_{ti} q^2 \sum_j p_{i,j} \bar{r}_j^{\,2} / 6kT \,. \tag{11}$$

3. Simulation results

Three model localised state distributions were used in this study. The first was a broad exponential tail of characteristic energy 50 meV. The other two represented respectively, low quality and a standard quality a-Si:H. In both cases, a band-tail energy parameter of 30 meV was used. Both include also a defect 'bump' centred at 0.65 eV below the conduction band edge, of half – width 60 meV, as found in TPC experiments [7]. In the former case, labelled 'DOS#1', the peak density was 2×10^{18} cm^{-3}eV^{-1}, while in the latter, 'DOS#2', a value of 2×10^{17} cm^{-3}eV^{-1} was used. Common values for other parameters used, are $\nu = \nu_0 = 10^{12}$ Hz, $\mu_{ext} = 10$ cm^{2}V^{-1}s^{-1}, $g(E_C) = 4 \times 10^{21}$ cm^{-3}eV^{-1} and $R_0 = 5 \times 10^{-8}$cm. We use a system of 72 levels, extending to 1.0 eV below the conduction band edge.

Fig. 1 shows the computed *i(t)* vs *t* for the case of the broad exponential tail, at 200 K, for MT-only transport and for MT+hopping transport. It can be seen that the introduction of hopping makes very little difference to the shape or magnitude of the total photocurrent decay, although the free carrier component is markedly reduced when hopping occurs. It is also of interest to note that the MT decay component, although two orders of magnitude below the hopping current, also follows the *same* overall power-law slope.

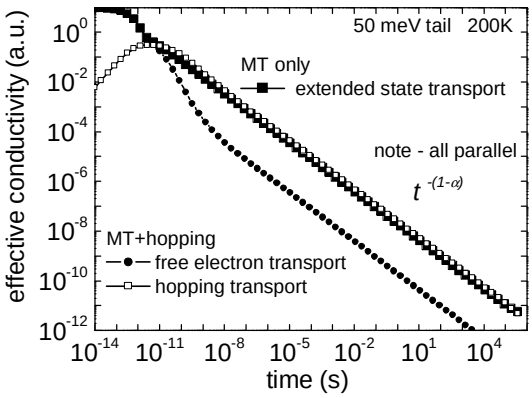

Fig. 1. Computed photocurrent decay curves for a 50 meV tail at T = 200 K, for the cases of MT-only and MT+hopping.

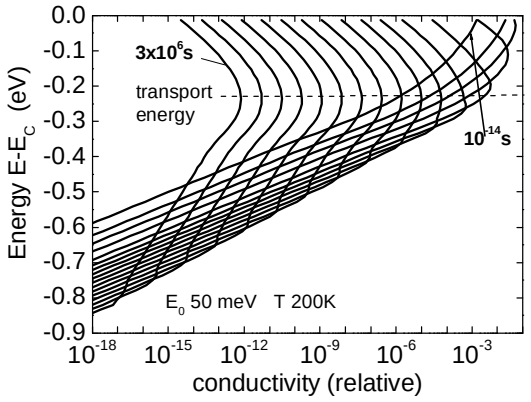

Fig. 2. Profile of the hopping current distribution at equal logarithmic time intervals, for a 50 meV tail at T = 200 K.

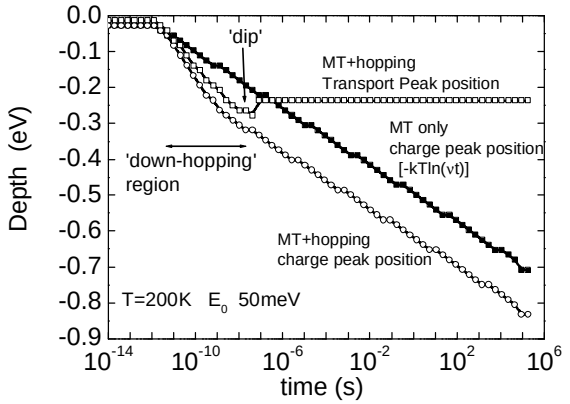

Fig. 3. Progress of the peak of the charge distribution and peak transport energy with time, for a 50 meV tail, at T=200 K

Fig. 2 shows the evolution of the energy distribution of the hopping current (strictly, the low-field conductivity) at equal logarithmic time intervals, from 10^{-14} to 3×10^6 s. After an initial 'hopping-down' regime, the transport peak settles at a 'transport energy' E_t = 0.236 eV below E_C, in reasonable agreement with the value of 0.244eV predicted by Monroe [1], *viz.*,

$$E_t = 3kT_0 \ln(T_0/T) - kT_0 \ln\left(1/\left(27R_0^3 N_C kT_0\right)\right). \quad (12)$$

We note from Fig. 3 that the instantaneous hopping transport energy peak exhibits a short-time 'dip' below its final value of E_t. Such a feature is common to most of the simulations in this work. Examination of Fig. 2 reveals the reason. The energy distribution of hopping transport contains two local features; a fixed maximum at E_t, and a descending feature related to the position of the density peak in the thermalising charge packet, the so called 'thermalisation demarcation energy', $E_d(t)$. When $E_d(t)$ has descended just below E_t, the increased density of charge at this energy results in a temporary downward shift of the position of peak hopping transport.

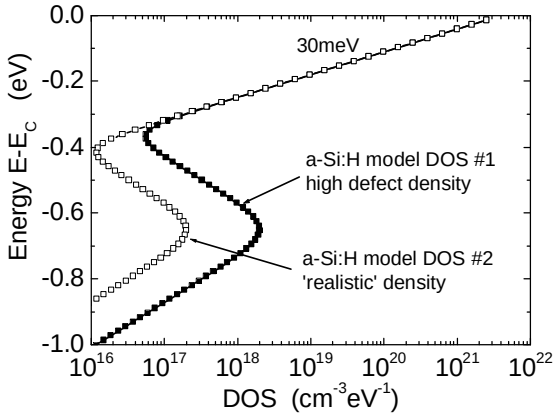

Fig. 4. Model density of states used in the simulations.

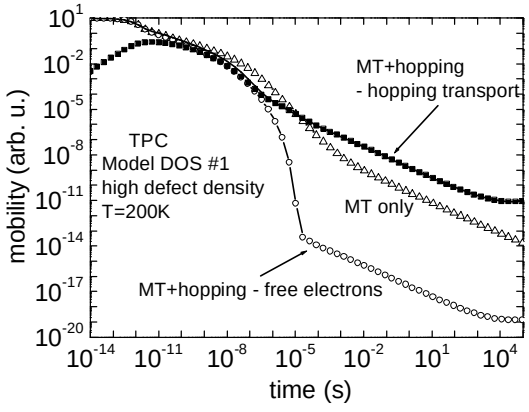

Fig. 5. Transient decay of photocurrent components. MT-only and MT+hopping, for DOS #1, at T=200 K.

Fig. 4 shows the two model densities of states used to represent poor and standard quality a-Si:H in this study. Both have a band-tail of 30 meV slope and a defect 'bump' at 0.65 eV depth,

while there is a factor of 10 difference in the densities of defects. Fig. 5 shows the simulated transient photocurrent components - extended state and hopping - for the MT-only and MT+hopping cases. In the case of 'MT-only' transport, the decay first shows thermalisation down the band tail, and then a drop of 4 orders of magnitude starting at 10^{-7}s, corresponding to the capture of electrons in the defect states. When hopping is included in the simulation, the density of free carriers falls much more drastically, and at a shorter time, as carriers move down by hopping to the defects, but the observed current does not fall so markedly. Indeed, the hopping current now exceeds the current for the MT-only case. Again, the long time slopes for the two cases are equal.

Figs. 6 and 7 show how the positions of the charge and transport peaks move during thermalisation. In the MT case, at about 10^{-7} s, deep trapping shifts the thermalising peak to 0.65 eV, where it remains until 10^{4} s. When hopping is included, the shift occurs earlier, at around 10^{-8}s, and hopping then forces the peak to continue downwards soon afterward. The transport energy remains in the band-tail for some time after the charge transfers to the defects, but then itself makes a rapid downward transition. It is of interest to note that a second 'down-hopping' region occurs, with another 'dip', before a new transport energy is established within the defects.

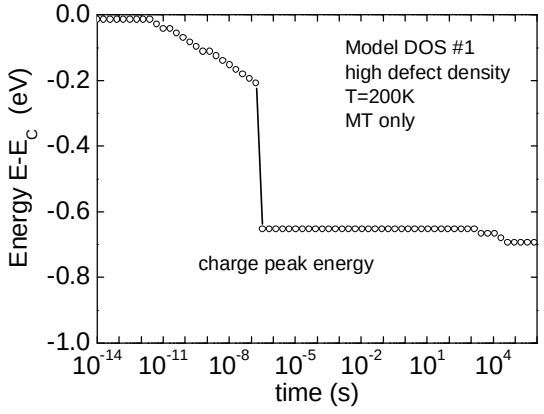

Fig. 6. Position of the thermalising charge for DOS#1 at 200K. MT-only case.

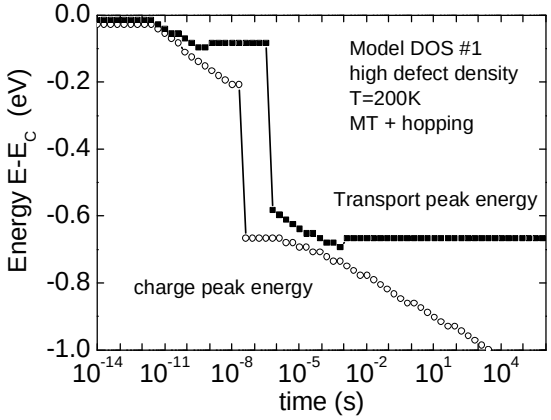

Fig. 7. Positions of the thermalising charge and transport energy for DOS#1 at 200 K. MT+hopping case.

Fig. 8 shows simulated TPC curves for the a-Si:H 'DOS$^{\#}$2' case, for MT-only and MT+hopping, at 300 K and 100 K. Intermediate temperature curves have been omitted, for clarity. We note that at 300 K, with the realistic parameters used, the computed current when hopping is included is very close to the MT-only current, with only a slightly faster deep trapping 'turn-down'. MT transport still dominates, but hopping slightly speeds up the thermalisation in this case. At 100K, hopping transport dominates at all times greater than 10^{-12}s, though the hopping current falls below the MT-only current at long times. At this temperature, there appears no time region where the MT and hopping current decays are parallel.

Fig. 9 illustrates the reconstruction of the DOS from the data of Fig. 8, using the Fourier transform technique developed by the authors for MT transport [3]. When only MT transport is considered, the reconstructed DOS matches the original model DOS reasonably well, at all temperatures. However, when the MT+hopping data are analysed in the same way, while the band-tail is reproduced reasonably well at all temperatures, the defect peak appears to move to shallower energies as the temperature is reduced.

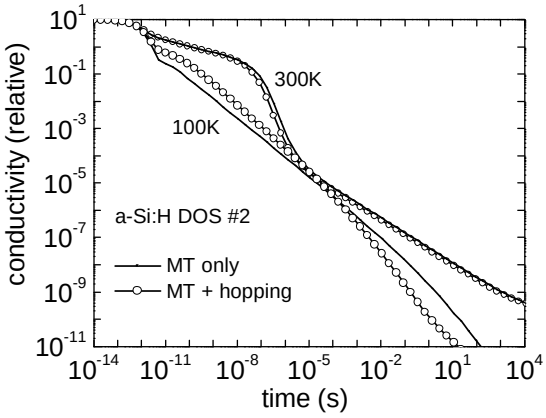

Fig. 8 Simulated TPC curves for a-Si:H DOS#2, for MT-only, and MT+hopping, at T=300 K and 100 K.

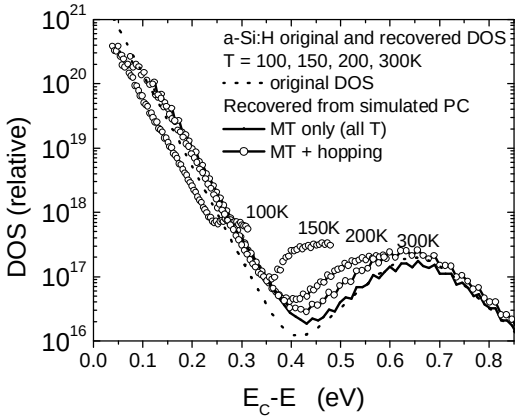

Fig. 9 DOS, reconstructed by the MT technique from the simulated data of Fig. 7, showing errors arising from non-inclusion of hopping.

4. Discussion

We have noted above that in many cases, the decay of the free electron current component is parallel to the decay of the dominant hopping current. However, the reverse has also been observed, *i.e.* parallel decays when the free electron current dominates. This phenomenon only occurs when the hopping transport has settled to a fixed transport energy, either near the band edge or within a defect level. Under these conditions, the thermalisation demarcation energy has descended below the hopping transport energy, and so the free carrier density 'tracks' the density at the hopping transport energy, since the occupancy of states *above* the demarcation energy is Boltzmann-like. Since the effective mobilities of the free and hopping carriers are constant under these conditions, the respective currents must also track each other, whichever is dominant. Thus, at the lowest temperatures, where 'hopping down' occurs over the whole simulated time range, the two components are never parallel.

It is also clear that with the addition of hopping, and under the above conditions, the peak in the charge distribution moves downward in energy on a path which parallels the $-kT\ln(\upsilon t)$ progress of the MT-only case (see Fig. 3). However, the *effective* frequency term describing the peak position, at around 2×10^{15} Hz, is much higher than the value of 10^{12} Hz used in the simulation. This may have implications for any energy scale associated with measured currents.

5. Conclusions

We have demonstrated a simple simulation technique for both MT-only and MT+hopping transport. It can model transient photo-responses for arbitrary distributions of states, over a very wide simulation time span, in a relatively short execution time. The simulation allows the contributions of extended state and hopping transport to be distinguished and their interaction to be studied. The influence of hopping on the MT-based interpretation of TPC to reconstruct the DOS has been demonstrated, and shown to have a possible influence at rather higher temperatures than hitherto expected.

Acknowledgments

C. M. and S. R. wish to acknowledge the management of the School of Computing and Advanced Technologies of the University of Abertay Dundee for their long term vision, and consistent level of support over the past several years, for this and other research projects of the

amorphous semiconductor group. J. M. M. wishes to thank the University of Wales Swansea, and in particular Professor B. Wilshire, for equivalent support for Swansea's Electronic Materials Centre. Sincere thanks are due to A. Osman Kodolbas, of the University of Haceteppe, Turkey, for the motivation for the present work.

References

[1] D. Monroe, Phys. Rev. Lett. **54**, 146 (1985).
[2] T. Tiedje, A. Rose, Sol. State Comm. **37**, 49 (1980).
[3] C. Main, D. Nesheva, J. Optoelectron. Adv. Mater. **3**, 655 (2001).
[4] J. M. Marshall, Philos. Mag. Lett. **80**, 691 (2000).
[5] J. M. Marshall, J. Mat. Sci.: Materials in Electronics **14**, 611 (2003).
[6] C. Main, J. Berkin, A. Merazga, in New Physical Problems in Electronic Materials ed. N. Kirov, A Vavrek, J.M. Marshall, World Scientific Press, Singapore, 1991, p 55.
[7] C. Main, R. Brüggemann, D. P. Webb, S. Reynolds, J. Non-Cryst. Solids, **165/166**, 481 (1993).